

Cite this: *Mater. Adv.*, 2023,  
4, 3192Received 19th May 2023,  
Accepted 13th July 2023

DOI: 10.1039/d3ma00251a

rsc.li/materials-advances

# Preparation of an amphipathic polymer library in a mixture of water/ethanol by photoinduced polymerization and evaluation of the cryoprotective activity†

Masanori Nagao,<sup>id</sup>\* Shuya Tanaka and Yoshiko Miura<sup>id</sup>\*

**Synthetic cryoprotectants with macromolecular structures are desirable as alternatives to commonly used ones. Herein, we prepared an amphipathic polymer library and evaluated the cryoprotective ability of the polymers by facile screening using red blood cells. The cryoprotective properties of the amphipathic polymers was independent of both the log *P* values of the hydrophobic groups and the ice recrystallization inhibition activity.**

Cryopreservation, the process of preserving materials at temperatures below 0 °C, is an essential process in food, clinical, and biomedical science.<sup>1–3</sup> To avoid damage to cells through recrystallization of the ice crystals during the cryopreservation, cryoprotectants are used. Dimethyl sulfoxide (DMSO) and glycerol are commonly used cryoprotectants.<sup>1</sup> These molecules interact with water molecules resulting in a decrease in the freezing point (water becomes a glassy state). However, because the action of these small-molecule cryoprotectants is colligative, a high concentration is required, which can cause cytotoxicity because these compounds can permeate the cell membrane. Organisms living in cold regions express antifreeze proteins (AFPs) to protect against the freezing of tissues at freezing temperature.<sup>4–8</sup> AFPs have the ability to control ice nucleation and growth. One of the function of AFPs is the inhibition of ice recrystallization, which is caused by the strong binding of AFPs on the surfaces of small ice particles.<sup>9–13</sup> AFPs are expected to be used as new cryoprotective materials to solve the problems of the currently used cryoprotective agents because of their high antifreeze activity and impermeability to cell membranes.<sup>1</sup> However, the extraction and purification of AFPs from natural sources are expensive, and alternative cryoprotectants that are easier to produce are desirable.

Antifreeze protein-mimetic materials made of synthetic polymers have been studied as alternative materials to natural AFPs. These mimetics do not permeate cell membranes and can protect cells when used in small amounts.<sup>14–20</sup> Previous reports by Gibson *et al.* have suggested that the presence of both hydrophilic and hydrophobic moieties in the same molecule (amphipathicity) in synthetic polymers is important for ice recrystallization inhibition (IRI) activity.<sup>21</sup> It has also been shown that the hydrophobic residues in antifreeze protein molecules are important for ice binding, and interaction with the cell membrane, in the cryoprotection of erythrocytes.<sup>22</sup> Therefore, amphipathic synthetic polymers may be excellent cryoprotectants. Different from the natural amino acids in protein polymers, there are a wide variety of hydrophobic functional groups that can be incorporated in synthetic polymers, and the ratios of different functional groups in the molecule can be easily controlled by the polymerization procedure. However, how the types and ratios of hydrophobic functional groups in amphipathic polymers affect the cryoprotective properties for the cell preservation is not well understood.

Herein, we comprehensively synthesized amphipathic polymers composed of hydrophilic and hydrophobic monomers using photoinduced electron/energy transfer-reversible addition-fragmentation chain transfer (PET-RAFT) polymerization.<sup>23–25</sup> Such photoinduced polymerization can enable the preparation of a library of polymers with various compositions at one time on a 96-well plate.<sup>26–32</sup> To enable sequential application to the screening of cryopreservation activity, we sought a polymerization solvent system for the amphipathic polymers that could be easily removed *in vacuo* after the reaction. Eosin Y, which is a photocatalyst for PET-RAFT polymerization, was dissolved in a mixture of water and ethanol (1/1 vol%) with the hydrophilic monomer (*N,N*-dimethylacrylamide; DMA), RAFT agent, and an amine compound (triethylamine or triethanolamine). The polymerization proceeded under irradiation of green light ( $\lambda = 527$  nm) without degassing. Triethanolamine provided better control of dispersity at a high conversion rate than triethylamine (Fig. S1 and Table S1, ESI†). The rate of the polymerization reaction was dependent on

Department of Chemical Engineering, Kyushu University, 744 Motoooka, Nishi-ku, Fukuoka 819-0395, Japan. E-mail: nagaom@chem-eng.kyushu-u.ac.jp, miuray@chem-eng.kyushu-u.ac.jp

† Electronic supplementary information (ESI) available. See DOI: <https://doi.org/10.1039/d3ma00251a>



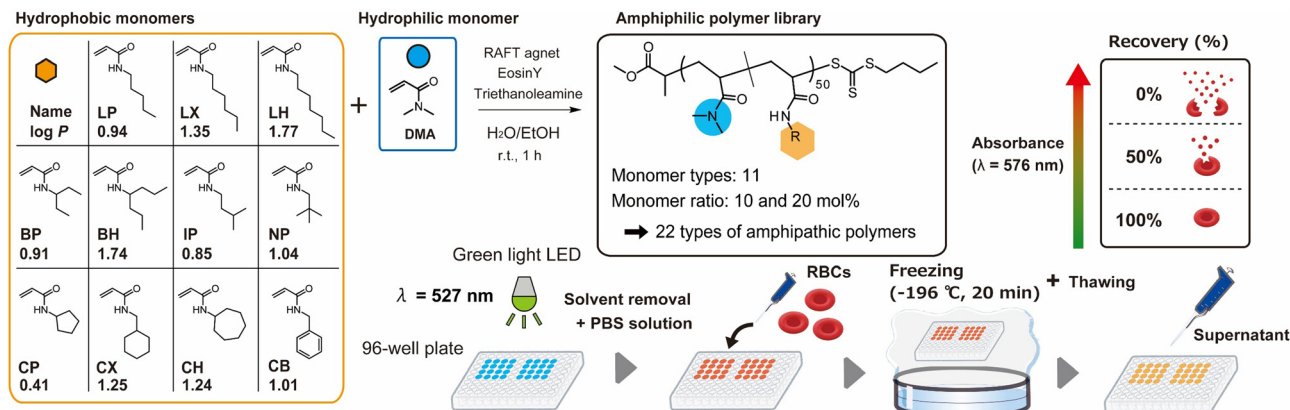


Fig. 1 Schematic illustration of the preparation of an amphipathic polymer library by PET-RAFT polymerization.

the equivalents of triethanolamine in the system, indicating that triethanolamine generated a radical species to start the polymerization in combination with excited Eosin Y (Fig. S1, ESI<sup>†</sup>). To avoid an excess amount of generated radical species, the use of one equivalent of triethanolamine to the RAFT agent was determined to be optimal for the reaction.

A library of amphipathic copolymers was prepared in a 96-well plate under the optimal conditions determined above. A total of 11 hydrophobic monomers with linear, branched, and cyclic hydrogen carbon chains, each with 5, 6, or 7 carbons in the chain were selected (Fig. 1). These hydrophobic monomers had different hydrophobicity, as described by the log *P* values. Each hydrophobic monomer was designated as a two-letter alphabetic abbreviation. In each well, DMA and the hydrophobic monomers were dissolved at various ratios and polymerized by light irradiation for 60 min. Polymers with various monomer compositions (DMA: hydrophobic monomers) were prepared in each well. To ensure the solubility of the amphipathic polymers during the polymerization, the target degree of polymerization was set as 50. Because some of the reaction solutions became cloudy or viscous at more than 30 mol% of hydrophobic monomer, because of the insolubility of the amphipathic polymers in the cosolvent system, the library was composed of 10 and 20 mol% of hydrophobic monomers (Table 1). Conversion ratios were over 90% for all the polymers, except **20CX**. Size exclusion chromatography (SEC) analysis revealed that dispersity range of the obtained polymers was relatively narrow. Although the polymer containing 20 mol% of *N,N*-heptylacrylamide (**20LH**) showed a non-unimodal peak because of the high hydrophobicity of **LH**, the other polymers showed the unimodal peaks indicating that the PET-RAFT copolymerization was well controlled (Fig. S2, ESI<sup>†</sup>).

The cryoprotective property of the synthesized polymers was evaluated by a cryopreservation test using red blood cells (RBCs).<sup>26</sup> A samples of the polymer solution (40  $\mu\text{L}$ ) in each well was added to a microtube, and the solvent was dried *in vacuo*. The residual solids were redissolved in PBS solution to give a polymer concentration of 10  $\text{g L}^{-1}$ . The polymer solution and the RBC suspension were mixed (60  $\mu\text{L}$  each, a total of 120  $\mu\text{L}$  per well) and frozen using liquid nitrogen

vapour for 20 min. The frozen samples in the plates were immediately thawed in an incubator (45  $^{\circ}\text{C}$  for 15 min), and RBCs in the wells were precipitated by centrifugation. The supernatants were mixed with AHD solutions in another plate, and haemolysis was evaluated by measuring the absorbance at 576 nm on a plate reader. The percent recovery of the RBCs with the polymers was calculated, and the values were summarized in a heat map (Fig. 2). Although the additives in the polymerization solution were not purified, those did not affect the cryoprotective activity (Table S2, ESI<sup>†</sup>). DMA homopolymer (**PolyDMA**) and **10NP** (consisting of 10 mol% of neopentyl acrylamide) showed the highest value of the compounds in the polymer library (RBC recovery = 70 and 71%, respectively). These values were higher than those of DMSO and glycerol at the same concentration (10  $\text{g L}^{-1}$ ; RBC recoveries were 63% and 46%, respectively), suggesting that those polymers are effective cryoprotectants for RBCs. Although we anticipated that the cryoprotective activity of amphipathic polymers would be related to the log *P* values of the hydrophobic monomers, the plots of percent recovery *versus* the log *P* values of the hydrophobic monomers showed no correlation (Fig. S4, ESI<sup>†</sup>). This result indicated that there must be another factor that determines the cryoprotective properties of the polymers. Dynamic light scattering measurements demonstrated that the polymers were dissolved in PBS solution as single molecules, except **10LP** (Table 1 and Fig. S3, ESI<sup>†</sup>), and thus involvement of the influence of self-assembly of the amphipathic polymers was eliminated.

To examine the mechanism for the cryoprotection of the RBCs, the IRI activity of the polymers was evaluated by the “splat-cooling” assay.<sup>33–35</sup> Solutes with IRI activity reduce the size of ice crystals during annealing at sub-zero temperatures ( $-8\text{ }^{\circ}\text{C}$ ). The mean largest grain size (MLGS) of the synthesized polymer showing the highest percent recovery of RBCs (**10NP**) was 79% (relative to PBS control) at 10  $\text{g L}^{-1}$  after annealing for 30 min (Fig. 3 and Table S2, ESI<sup>†</sup>). Considering the MLGS of **10LP** (86%) and **10CP** (106%), which showed a low percent recovery, these results suggested that the cryoprotective properties of **10NP**, **10LP**, and **10CP** did not depend on the IRI activity (Fig. 3). It should be noted that these MLGS values were



Table 1 Amphipathic polymer library prepared by PET-RAFT polymerization<sup>a</sup>

Polymer	Hydrophobic monomer ratio <sup>b</sup> (mol%)	Conv. <sup>b</sup> (%)	$M_{n,SEC}$ <sup>c</sup> (g mol <sup>-1</sup> )	$M_{w,SEC}$ <sup>c</sup> (g mol <sup>-1</sup> )	$M_w/M_n$ <sup>c</sup>	$D^d$ (nm)
10LP	10	93	1700	2300	1.32	102 ± 2
20LP	20	93	3700	4800	1.30	5.8 ± 0.5
10LX	10	95	2000	2400	1.25	4.6 ± 0.1
20LX	20	95	3800	5700	1.50	7.1 ± 0.1
10LH	10	95	2100	3000	1.40	7.8 ± 0.3
20LH	20	94	4200	6800	1.61	10.7 ± 0.2
10BP	10	97	2200	3000	1.39	4.3 ± 0.1
20BP	20	95	4100	5500	1.33	4.5 ± 0.1
10BH	10	95	2100	3000	1.46	4.9 ± 0.7
20BH	20	92	4200	5600	1.35	10.5 ± 0.3
10IP	10	93	1800	2300	1.29	3.8 ± 0.3
20IP	20	94	4300	5700	1.30	4.6 ± 0.2
10NP	10	96	1800	2200	1.24	4.0 ± 0.2
20NP	20	90	4300	5500	1.28	4.5 ± 0.1
10CP	10	95	1900	2300	1.23	4.5 ± 0.2
20CP	20	95	3700	5000	1.35	5.6 ± 0.1
10CX	10	95	1900	2500	1.33	5.4 ± 0.2
20CX	20	81	4100	5200	1.29	7.9 ± 0.3
10CH	10	95	2400	3100	1.27	5.5 ± 0.1
20CH	20	91	3900	5200	1.36	6.6 ± 0.7
10CB	10	95	2000	2400	1.23	5.2 ± 0.2
20CB	20	90	4000	5100	1.28	4.6 ± 0.2

<sup>a</sup> Monomer concentration was 1 M in H<sub>2</sub>O:EtOH (1:1). <sup>b</sup> Monomer conversion and incorporated ratio of the hydrophobic monomers were determined by <sup>1</sup>H NMR measurements. <sup>c</sup> Molecular weight and dispersity were determined by SEC analysis (*N,N*-dimethylformamide with 10 mM LiBr as eluent) calibrated to a polymethylmethacrylate standard. <sup>d</sup> Hydrodynamic diameter was determined by dynamic light scattering (10 g L<sup>-1</sup> in PBS at 25 °C).

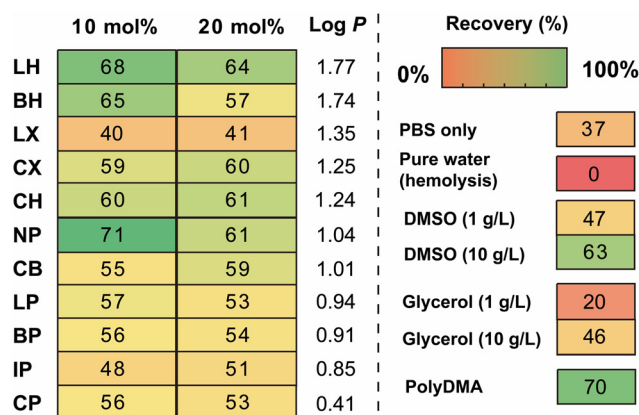


Fig. 2 Heat map showing post-thaw RBCs recovery outcomes using 10 g L<sup>-1</sup> of polymer. Recoveries are the average of three repeats.

higher than that of polyvinyl alcohol, which is a representative IRI active polymer (MLGS less than 20% at ≥ 0.5 g L<sup>-1</sup>),<sup>35</sup> suggesting that the IRI activity of the synthesized amphipathic polymers was not high.

Next, the interaction of the amphipathic polymers and RBCs was evaluated. Meister and co-workers have reported that the interaction of antifreeze proteins with the cell membrane is important for the cryopreservation of cells through the stabilization of the membrane structure under physical stress.<sup>36</sup> We propose that such an interaction of the synthesized amphipathic polymers with the membranes of RBCs may be involved in the cryoprotective property. However, the interactions of the amphipathic polymers with cell membranes may cause damage to the cells. Thus, we evaluated the cytotoxicity of the polymers

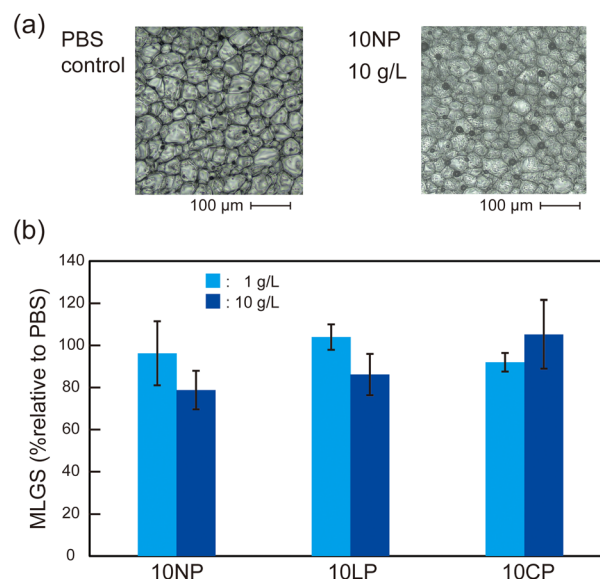


Fig. 3 Ice recrystallization inhibition activity of the amphipathic polymers as measured by the splat assay. (a) Example micrographs showing ice crystals grown in PBS alone (left) and with **10NP** (10 g L<sup>-1</sup>, right); (b) Mean largest grain size (MLGS) of each polymer relative to a PBS control, expressed as %. Error bars represent the standard deviation from at least three measurements.

towards RBCs during incubation. After incubation for 2 h at room temperature, the amphipathic polymers containing hydrophobic groups with high log *P* values (> 1.24) showed collapse RBCs even with a 10 mol% ratio of hydrophobic groups (Fig. 4). The polymers with 20 mol% of hydrophobic monomers showed a higher percentage of collapsed RBCs. This result



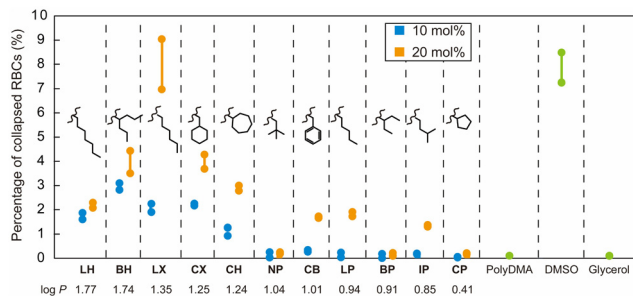


Fig. 4 Cytotoxicity of the amphipathic polymers toward RBCs after incubation for 2 h at room temperature ( $n = 2$ ). Concentration of the solutes was  $10 \text{ g L}^{-1}$ .

indicated that the incorporated hydrophobic groups enhanced the interaction of the polymers with the cell membranes of the RBCs, resulting in the release of haemoglobin. Although both **NP** and **BP** polymers showed no cytotoxicity towards RBCs, the percent recoveries of RBCs in the cryopreservation test of **NP** polymers were higher than those of **BP** polymers. This result indicated that moderate hydrophobicity of the amphipathic polymers was effective for cryoprotective activity.

In conclusion, an amphipathic polymer library was prepared by photoinduced polymerization in a mixture of water and ethanol, and the samples were evaluated in a cryopreservation test using RBCs. The polymers containing a 10 mol% of *N*-neopentylacrylamide (**10NP**) showed the highest percent recovery of RBCs among the synthesized polymers, and this value was higher than those of DMSO and glycerol at a concentration of  $10 \text{ g L}^{-1}$ . Subsequent evaluation revealed that neither the log *P* value of the hydrophobic groups nor the IRI activity was correlated with the cryopreservation activity. Several papers are suggesting other mechanisms as key factors in cryopreservation (e.g., the interactions with cell membranes<sup>36</sup> and dehydration process during freezing<sup>37,38</sup>). Further investigation of amphipathic polymers synthesized using controlled polymerization techniques is required to reveal the correlation between the polymer structures and the cryoprotectant activity.

## Author contributions

The experiments were planned by M. Nagao and conducted by S. Tanaka. The manuscript was written by M. Nagao. Y. Miura provided discussion and advice to improve the quality of the research.

## Conflicts of interest

There are no conflicts to declare.

## Acknowledgements

This work was supported by the Asahi Glass Foundation and JSPS (22K14728, 22H05430, 22H05048, 19H02766).

## References

- Z. Liu, X. Zheng and J. Wang, *J. Am. Chem. Soc.*, 2022, **144**, 5685–5701.
- K. A. Murray and M. I. Gibson, *Nat. Rev. Chem.*, 2022, **6**, 579–593.
- T. Chang and G. Zhao, *Adv. Sci.*, 2021, **8**, 2002425.
- Y. Tachibana, G. L. Fletcher, N. Fujitani, S. Tsuda, K. Monde and S.-I. Nishimura, *Angew. Chem., Int. Ed.*, 2004, **43**, 856–862.
- M. B. Dolev, I. Braslavsky and P. L. Davies, *Annu. Rev. Biochem.*, 2016, **85**, 515–542.
- A. Bialkowska, E. Majewska, A. Olczak and A. Twarda-Clapa, *Biomolecules*, 2020, **10**, 274.
- A. Baskaran, M. Kaari, G. Venugopal, R. Manikkam, J. Joseph and P. V. Bhaskar, *Int. J. Biol. Macromol.*, 2021, **189**, 292–305.
- H. Xiang, X. Yang, L. Ke and Y. Hu, *Int. J. Biol. Macromol.*, 2020, **153**, 661–675.
- S. Ebbinghaus, K. Meister, B. Born, A. L. DeVries, M. Gruebele and M. Havenith, *J. Am. Chem. Soc.*, 2010, **132**, 12210–12211.
- A. Hudait, Y. Qiu, N. Odendahl and V. Molinero, *J. Am. Chem. Soc.*, 2019, **141**, 7887–7898.
- S. Chakraborty and B. Jana, *J. Phys. Chem. B*, 2018, **122**, 3056–3067.
- K. Mochizuki and V. Molinero, *J. Am. Chem. Soc.*, 2018, **140**, 4803–4811.
- Y. Sun, G. Giubertoni, H. J. Bakker, J. Liu, M. Wagner, D. Y. W. Ng, A. L. Devries and K. Meister, *Biomacromolecules*, 2021, **22**, 2595–2603.
- I. K. Voets, *Soft Matter*, 2017, **13**, 4808–4823.
- C. I. Biggs, C. Stubbs, B. Graham, A. E. R. Fayter, M. Hasan and M. I. Gibson, *Macromol. Biosci.*, 2019, **19**, 1900082.
- M. Gore, A. Narvekar, A. Bhagwat, R. Jain and P. Dandekar, *J. Mater. Chem. B*, 2022, **10**, 143–169.
- M. Hasan, A. E. R. Fayter and M. I. Gibson, *Biomacromolecules*, 2018, **19**, 3371–3376.
- C. Stubbs, T. L. Bailey, K. Murray and M. I. Gibson, *Biomacromolecules*, 2020, **21**, 7–17.
- V. Haridas and S. Naik, *RSC Adv.*, 2013, **3**, 14199–14218.
- C. I. Biggs, T. L. Bailey, B. Graham, C. Stubbs, A. Fayter and M. I. Gibson, *Nat. Commun.*, 2017, **8**, 1546.
- B. Graham, A. E. R. Fayter, J. E. Houston, R. C. Evans and M. I. Gibson, *J. Am. Chem. Soc.*, 2018, **140**, 5682–5685.
- R. Rajan, F. Hayashi, T. Nagashima and K. Matsumura, *Biomacromolecules*, 2016, **17**, 1882–1893.
- T. G. McKenzie, Q. Fu, M. Uchiyama, K. Satoh, J. Xu, C. Boyer, M. Kamigaito and G. C. Qiao, *Adv. Sci.*, 2016, **3**, 1500394.
- J. Phommalsack-Lovan, Y. Chu, C. Boyer and J. Xu, *Chem. Commun.*, 2018, **54**, 6591–6606.
- S. Shanmugam, J. Xu and C. Boyer, *J. Am. Chem. Soc.*, 2015, **137**, 9174–9185.
- C. Stubbs, K. A. Murray, T. Ishibe, R. T. Mathers and M. I. Gibson, *ACS Macro Lett.*, 2020, **9**, 290–294.



- 27 C. Stubbs, T. Congdon, J. Davis, D. Lester, S.-J. Richards and M. I. Gibson, *Macromolecules*, 2019, **52**, 7603–7612.
- 28 G. Ng, J. Yeow, R. Chapman, N. Isahak, E. Wolvetang, J. J. Cooper-White and C. Boyer, *Macromolecules*, 2018, **51**, 7600–7607.
- 29 S. Schaefer, T. T. P. Pham, S. Brunke, B. Hube, K. Jung, M. D. Lenardon and C. Boyer, *ACS Appl. Mater. Interfaces*, 2021, **13**, 27430–27444.
- 30 P. R. Judzewitsch, L. Zhao, E. H. H. Wong and C. Boyer, *Macromolecules*, 2019, **52**, 3975–3986.
- 31 M. Nagao, T. Uemura, T. Horiuchi, Y. Hoshino and Y. Miura, *Chem. Commun.*, 2021, **57**, 10871–10874.
- 32 M. Nagao, Y. Kimoto, Y. Hoshino and Y. Miura, *ACS Omega*, 2022, **7**, 13254–13259.
- 33 C. A. Knight, J. Hallett and A. L. DeVries, *Cryobiology*, 1988, **25**, 55–60.
- 34 S. Abraham, K. Keillor, C. J. Capicciotti, G. E. Perly-Robetson, J. W. Keillor and R. N. Ben, *Cryst. Growth Des.*, 2015, **15**, 5034–5039.
- 35 T. Congdon, R. Notman and M. I. Gibson, *Biomacromolecules*, 2013, **14**, 1578–1586.
- 36 Y. Sun, D. Maltseva, J. Liu, T. Hooker II, V. Mailänder, H. Ramløv, A. L. DeVries, M. Bonn and K. Meister, *Biomacromolecules*, 2022, **23**, 1214–1220.
- 37 K. Matsumura, F. Hayashi, T. Nagashima, R. Rajan and S.-H. Hyon, *Commun. Mater.*, 2021, **2**, 1–12.
- 38 A. A. Burkey, A. Hillsley, D. T. Harris, J. R. Baltzegar, D. Y. Zhang, W. W. Sprague, A. M. Rosales and N. A. Lynd, *Biomacromolecules*, 2020, **21**, 3047–3055.

